Electronic Supplementary Material (ESI) for Nanoscale.

Supporting Information

Ultrathin Ta_2O_5 Electron-Selective Contacts for High Efficiency InP Solar Cells

Parvathala Reddy Narangari[1], Siva Krishna Karuturi[1, 2]*, Yiliang Wu[2], Jennifer Wong Leung[1], Kaushal Vora[3], Mykhaylo Lysevych[1], Yimao Wan[2], H. H. Tan[1], C. Jagadish[1] and S. Mokkapati[3, 4]*

[1] Department of Electronic Materials Engineering, Research School of Physics and Engineering, Australian National University, Canberra, ACT 2601, Australia.

[2] Research School of Engineering, Australian National University, Canberra, ACT 2601, Australia.

[3] School of Physics and Astronomy, Cardiff University, Parade, Cardiff, United Kingdom, CF24 3AA

[4] Department of Materials Science and Engineering, Faculty of Engineering, Monash University, Victoria 3800 (Australia)

* Corresponding authors: siva.karuturi@anu.edu.au and Sudha.Mokkapati@Monash.edu

1. Solar cell fabrication

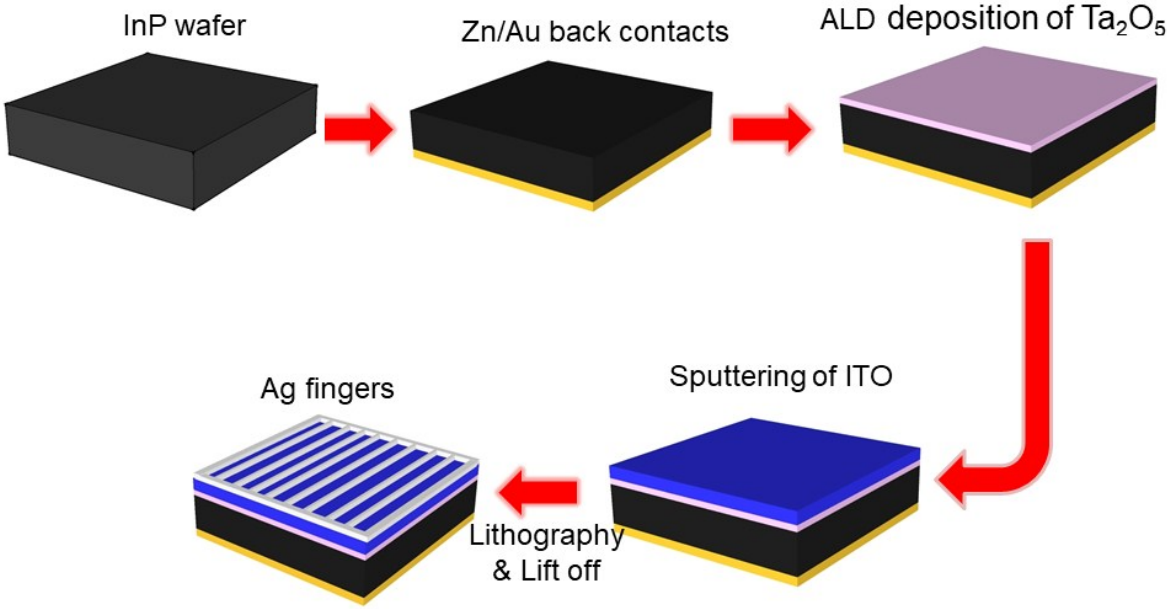

Figure s1. Processing steps involved in the fabrication of Ta_2O_5/InP heterojunction solar cell.

2. TEM and EDX mapping

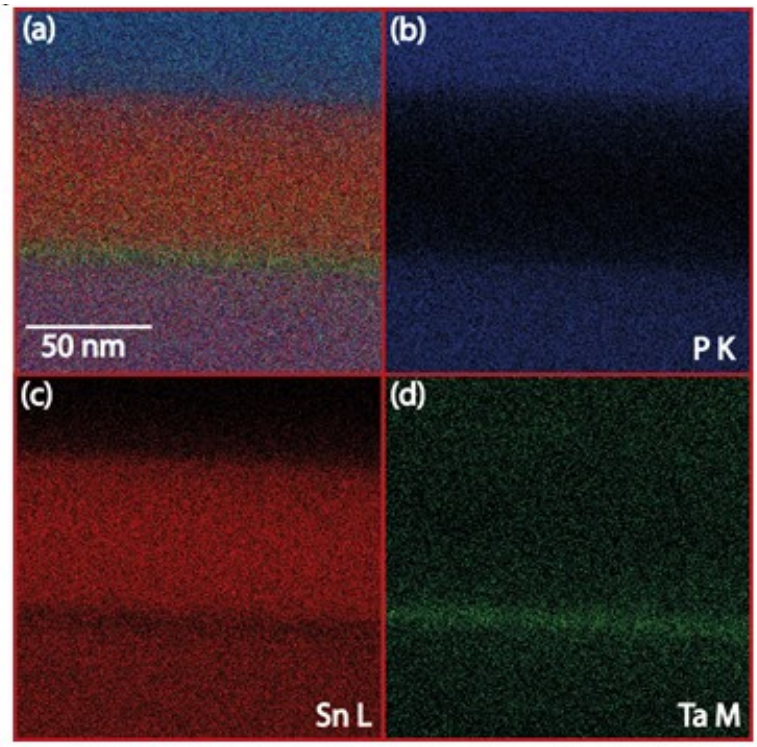

Figure s2. (a) False colour image of EDS mapping on Pt- ITO-Ta_2O_5-InP cross-section with the (b) P K map shown in blue, (c) the Sn L map shown in red and (d) the Ta M map shown in green.

High resolution transmission electron microsocpy (HRTEM) and electron dispersive x-ray spectroscopy (EDS) analysis were employed to analyze the structural properties and elemental analysis of Ta_2O_5 layer in the solar cell. Figure 1 of the manuscript shows the cross-section HRTEM image of the ITO-Ta_2O_5-InP interfaces. The elemental mapping of Pt-ITO-Ta_2O_5-InP interface is shown in Figure s2. Thick Pt film was deposited on top of ITO-Ta2O5-InP to avoid the ion damage during the TEM sample preparation using FIB. These measurements were carried out in scanning transmission electron microscope (STEM) mode with each elemental map extracted from the integrated intensity of the elemental peak at each point in the STEM image as shown in Figure s2(b)-(d). The false colour image in Figure s2(a) is an overlay of the P, Sn and Ta elemental mapping images (Figure s2b-d) of the device cross-section and confirms the presence of a uniform Ta_2O_5 layer in the device. The Pt layer shows a high P K intensity due to the fact that Pt Alpha (2.012eV) EDS peak is close to the P K Alpha (2.048eV).

3. InP-ITO and InP-Ta2O5-ITO interface characteristics

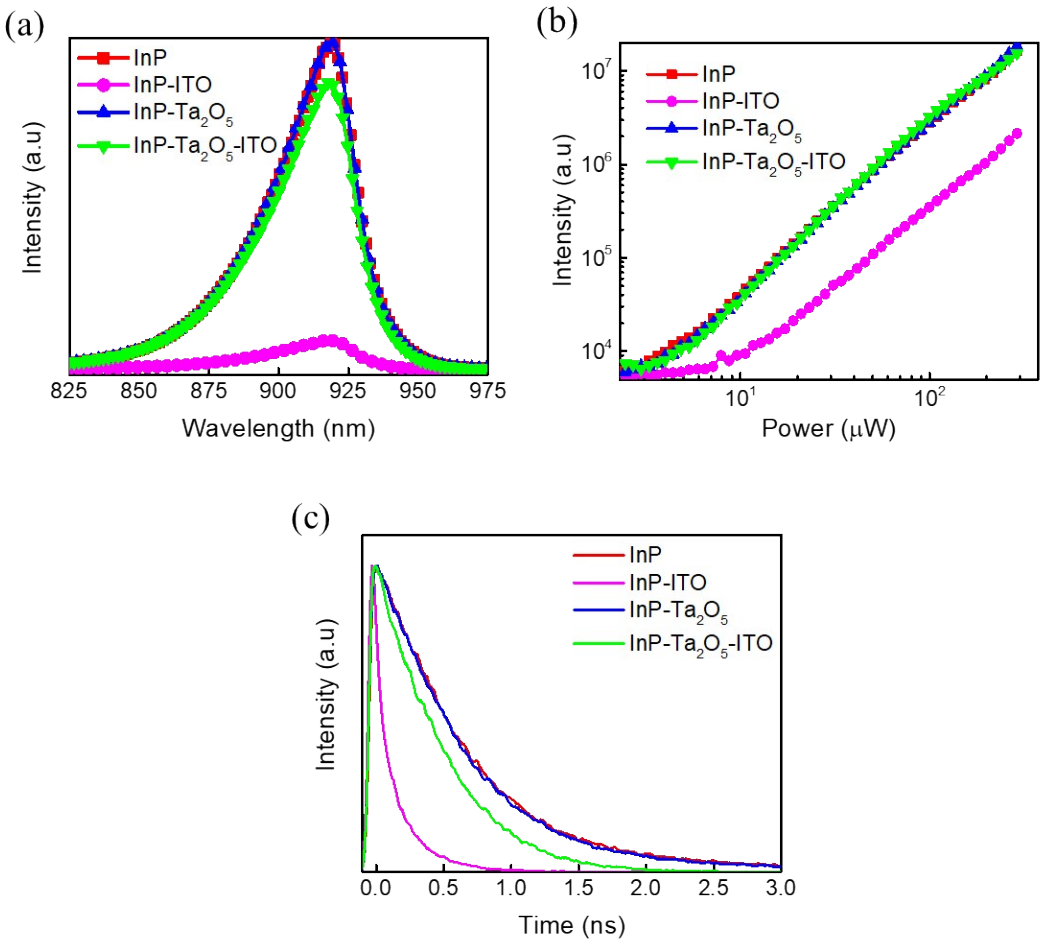

Figure s3. (a) Photoluminescence (PL) spectra, (b) PL peak intensity versus excitation power and (c) time resolved PL spectra for bare InP, InP-ITO, InPTa_2O_5 and InP-Ta_2O_5-ITO samples.

Figure s3(a) shows the photoluminescence (PL) spectra for bare InP, InP-ITO, InP- Ta_2O_5 and InP-Ta_2O_5-ITO samples. The thickness of the Ta_2O_5 layer is 8 nm. The bare InP sample and the InP-Ta_2O_5 sample have the same PL peak intensity. The PL intensity is drastically reduced for the InP-ITO sample, possibly due to surface damage. The PL peak intensity is almost recovered in the InP-Ta_2O_5-ITO sample, suggesting that the presence of Ta_2O_5 on InP surface prevents/reduces the surface damage caused by sputter deposition of ITO. Similar trend in PL peak intensities is maintained for the samples for excitation powers up to $3*10^2$ μW (Figure s3(b)).

Bare InP and InP- Ta_2O_5 samples also show very similar behavior in the time-resolved PL spectra (Figure s3(c)). Table s1 lists the minority carrier lifetimes extracted from the data shown in Figure s3(c). Bare InP and InP- Ta_2O_5 samples have minority carrier lifetime of 673

and 650 ps, respectively. The minority carrier lifetime in the InP-ITO sample is 138 ps, indicative of surface damage. As discussed above, presence of a Ta_2O_5 interlayer between InP and ITO reduces the surface damage, resulting in minority carrier lifetime of 494 ps.

Table s1. Minority carrier lifetime for the different samples studied in this work.

Layer Structure	Minority carrier lifetime (ps)
InP	673
Ref (InP-ITO)	138
InP-5 nm Ta_2O_5	630
InP-8 nm Ta_2O_5	650
InP-12 nm Ta_2O_5	672
InP-8 nm Ta_2O_5-ITO	494

4. Dark J-V characteristics

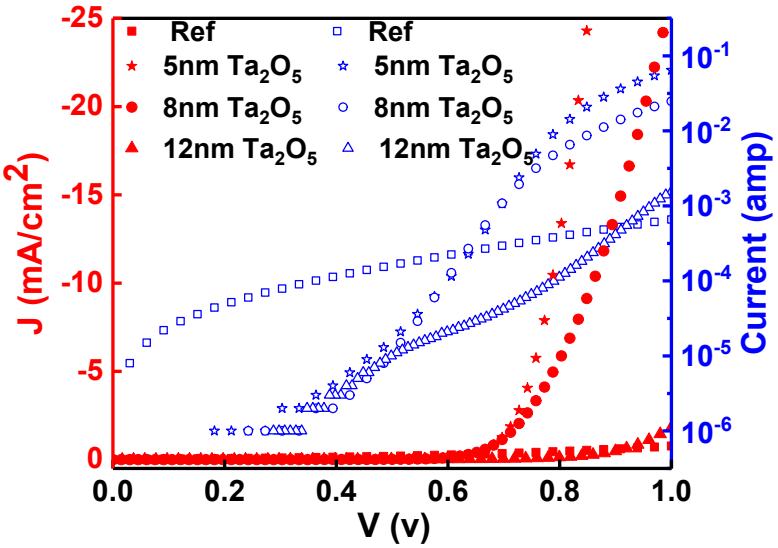

Figure s4. Dark J-V characteristics for reference (InP-ITO) and InP- Ta_2O_5-ITO solar cells.

Figure s4 shows the dark J-V characteristics of the reference (InP-ITO) and InP- Ta_2O_5-ITO solar cells. The effect of non-ideal shunt resistance is seen as departure from linear behavior at low currents in the log J vs V plot for the reference solar cell. On the other hand, the effect of series resistance is seen as departure from linear behavior at high currents in the log J vs V plot for both the InP-5 nm Ta_2O_5 and InP-8 nm Ta_2O_5 solar cells. We fit the linear region of log J vs V data to extract the reverse saturation current density, J_o, shown in Table s2. The J-V data for InP-12 nm Ta_2O_5 sample could not be fitted with a single diode equation.

Table s2. Reverse saturation current density, J_o, for the reference (InP-ITO) and InP-5/8 nm Ta_2O_5-ITO solar cells.

Device	**J_o**
Ref (InP-ITO)	37 μA/cm^2
InP-5 nm Ta_2O_5-ITO	60 nA/cm^2
InP-8 nm Ta_2O_5-ITO	0.1 nA/cm^2